FATIGUE ANALYSIS OF A PRESSURE VESSEL WELDED JOINT USING THE STRESS INTEGRATION METHOD OUTLINED IN THE ASME BOILER & PRESSURE VESSEL CODE VIII

A. Halfpenny[1], R. Plaskitt[2], J. Mentley[3], N.Mann[4]

A design challenge is to ensure the structural integrity of a pressure vessel to meet the regulatory requirements of the ASME Boiler & Pressure Vessel Code whilst minimizing material cost (wall thickness).

The paper describes the fatigue analysis of a welded joint in a pressure vessel subjected to road transport loading. It describes the method used to recover the stresses that are critical for this fatigue analysis using the commercial software nCode DesignLife.

Finite element analysis is used to calculate the structural stresses. The fatigue analysis uses detail stresses in the weld recovered using the stress integration method outlined in the ASME Boiler & Pressure Vessel Code VIII, Division 2. This method uses the structural stress at the location of interest, and the bending ratio associated with that stress. This avoids a specialized meshing scheme in the solid elements close to the weld.

INTRODUCTION

Metal fatigue typically occurs through long term exposure to time varying loads which, although modest in amplitude, give rise to microscopic cracks that can ultimately propagate to failure. Between 1852 and 1870, Wöhler [1] studied fatigue failure in railway axles using his rotating-bend fatigue rig. The rig housed two rotating shafts and, by applying different weights to the end of the rotating shafts, he was able to determine a relationship between the bending stress in the shaft and the number of rotations to failure. Subsequent work in 1910 by Basquin [2] recognized a logarithmic relationship between the amplitude of the sinusoidally varying stress and the number of rotations to failure. This work gave rise to the now familiar SN (or Wöhler) curve. Different materials were found to exhibit different characteristics and today it is customary to produce material-dependent Wöhler curves for use in design.

Whereas railway axles typically see sinusoidally varying loads, many other applications exhibit more random load profiles. In 1968, Mitsuishi and Endu [3] introduced an algorithm known as ‘Rainflow’ cycle counting which is used to extract fatigue cycles from a signal of time-varying stress. The algorithm extracts the range and mean stress for each fatigue cycle and the damage is computed with reference to the SN curve.

Dr A. Halfpenny, Chief Technologist, HBM-nCode, United Kingdom
Mr R. Plaskitt, Senior Engineer, HBM-nCode, United Kingdom
Mr J. Mentley, Senior Engineer, HBM-nCode, USA
Mr N. Mann, Engineer, Siemens UK

Further work by Palmgren [4] and Miner [5] showed how a reasonable estimate of the total damage could be obtained by summing the damage from each individual cycle.

Fatigue failures of welded joints also follow a familiar SN curve. In this case the micro structural properties of the material are heavily influenced by the welding process and so the performance of the base material has less effect on the SN curve of the weldment. In this case the curve is more heavily affected by weld geometry, residual stresses, penetration depth and general quality. Design standards such as BS7608 [6], Eurocode III [7] and ASME Pressure Vessel Code [8] classify weld SN curves with regard to their geometry while implicit account is taken of quality, penetration depth and residual stresses. In this case the design engineer must measure (or calculate) the nominal stress in the structural member ignoring the presence of the weld, and then use an SN curve appropriate to the geometry in order to determine the fatigue life. The curve implicitly accounts for the geometrical stress concentration.

In the case of complex joints it is often impractical to calculate or measure a 'nominal' stress. In this case the codes describe an alternative analysis process known as the 'hotspot' method. This attempts to measure the actual stress concentration caused by the weld so rather than having a family of SN curves we find they all collapse to a single curve. It is fair to say that many of the geometry classifications given in these codes relate to welds in large civil, offshore or heavy ground vehicle applications as well as welds in heavy pressure vessel structures. For example, the reference thickness in [6] is taken as 16mm. Little work is documented on their application to thin sheet structures such as light automotive or light-weight pressure vessels with wall thicknesses less than approximately 3mm.

With the advent of modern stress analysis techniques, guidance notes have been developed which recommend meshing techniques to obtain representative fatigue estimates using finite element analysis (FEA). International Institute of Welding [9] describes the application of FEA to the nominal stress approach and hotspot methods. It also describes how highly refined meshes can be applied to derive estimates based on both linear-elastic notch stresses and even more complex elastic-plastic notch strains. However, the use of these techniques is not applicable to general design of complex structures such as vehicle body-in-white or light-weight pressure vessels.

Nominal stress and hotspot techniques both require significant manual work in the form of selecting an appropriate weld geometry classification and then extracting stresses for subsequent analysis by hand calculation. This is straightforward, but time consuming, for constant amplitude loading, but is not practical for variable amplitude loading where fatigue cycles must be identified from time-varying stresses using Rainflow cycle counting. These limitations mean that both the nominal stress and hotspot techniques are not conducive to an automated FEA process with time-varying stresses.

Furthermore, the high mesh refinement required for the notch methods is not conducive to large-scale structural modeling of complex structures such as vehicle bodies, chassis or some pressure vessels. A more pragmatic approach is therefore required to allow standard FE meshing techniques to be used without recourse to hand calculations and this is the topic of this paper.

SEAM WELD ANALYSIS METHOD

The local notch stress at a welded joint can be considered as the sum of three components; these are membrane, bending and a non-linear stress peak, as illustrated in Figure 1. Membrane and bending stresses alone are attributable to the nominal stress in the component along with the effect of geometric stress risers. The non-linear stress peak is attributable to local weld effects such as geometry of the weld toe, penetration depth and varying weld quality. The nominal stresses are easily derived from FEA whereas the non-linear weld effects are far more complicated. The general approach to weld fatigue is to consider only the nominal stresses in design and allow the SN curves to inherently manage non-linear weld effects and statistical variability.

Fermér [10], working on fatigue analysis of car body structures, noticed that an entire family of weld SN curves could be collapsed to two master curves as illustrated in Figure 2. When membrane stresses are dominant at the weld toe the fatigue damage follows the lower SN curve; however, as bending stresses become dominant then the fatigue damage follows the upper SN curve. Subsequent work by nCode and Fermér derived an interpolation function between these two curves based on the ratio of bending stress to total stress as given in equation (1). The interpolation function is illustrated in Figure 3.

$$r = \frac{|\sigma_b|}{|\sigma_m| + |\sigma_b|} \tag{1}$$

Where r is the bending (or flex) ratio, σ_b is the bending stress and σ_m is the membrane stress.

The bending and membrane stresses are derived from FEA using a method given in [8], 2008a Annex 5, "Linearization of Stress Results for Stress Classification". This method integrates stress components along a user defined 'Stress Classification Line (SCL)' to determine membrane and bending stresses. The SCL is defined as a plane parallel to the weld toe as illustrate in Figure 4. The average membrane and bending stresses are calculated using equations (2) and (3) respectively.

$$\sigma_m = \frac{1}{t}\int_0^t \sigma(x)\, dx \tag{2}$$

$$\sigma_b = \frac{6}{t^2}\int_0^t \sigma(x)\left(\frac{t}{2} - x\right) dx \tag{3}$$

Where $\sigma(x)$ is the stress at depth x along vector V_t perpendicular to the weld line as illustrated in Figure 4.

For solid element meshes, the stresses $\sigma(x)$ are derived at discrete sub-surface nodes as illustrated in Figure 4. The top and bottom surface nodes are disregarded as these are most sensitive to local mesh discontinuities adjacent to the weld toe. FEA surface stresses are replaced with analytical stresses derived by extrapolation of the sub-surface values. This offers a significant degree of tolerance to mesh sensitivity which is

demonstrated in Figure 5. While the surface stresses adjacent to the weld toe vary by more than a factor of 2 with respect to mesh density, the analytically derived surface stresses vary by only 4.8%.

Residual stress effects are usually accounted for implicitly in the weld SN curve, however, it is useful to account for cyclic mean stress correction explicitly. In this analysis the FKM [11] mean stress correction factor is implemented as illustrated in the Haig diagram in Figure 6.

Component thickness also has an influence on fatigue damage. Fatigue strength decreases with increasing thickness. The thickness correction factor expressed in equation (4) is based on those used in [6] and [11] but also allows a choice of reference thickness as well as thickness exponent.

$$\text{If } t \geq t_{ref}, \text{ then } f_t = \left(\frac{t_{ref}}{t}\right)^n \qquad (4)$$

$$\text{Or if } t < t_{ref}, \text{ then } f_t = 1$$

Where f_t is the thickness correction factor, t is the actual thickness of the member, T_{ref} is the reference thickness or threshold, and n is the thickness exponent.

METHOD VALIDATION

A number of validation tests were performed to determine the accuracy of the method. Figure 7 shows the analysis of a simple T-specimen subjected to constant amplitude loads applied in both in- and out-of-plane bending. The analytical results were compared with those of TWI [12]. Fatigue life estimates reveal excellent correlation with measured test results as given in Table 1. All observed failure sites were predicted by the FEA as illustrated in Figure 8.

TABLE 1 – Comparison of FE fatigue estimates with measured test for T-specimen

	Measured life in cycles	FE Estimated life in cycles
In-plane loading	70,900 (15mm observed crack)	26,000
Out-of-plane loading	74,000	43,800

Further FEA validation tests were performed on a number of test specimens under constant amplitude loading. The results are shown in Figures 9 through 13 with measured test results compared with [12] and Auto Steel Partnership [13]. All results show excellent correlation with measured test data.

PRESSURE VESSEL CASE STUDY

One of the challenges faced by pressure vessel manufacturers is how to minimize material cost, for example, by reducing wall thicknesses. However any design changes must maintain the structural integrity of the vessel and meet the regulatory requirements of the ASME Boiler & Pressure Vessel Code. Computer simulations are used to assess potential design changes to identify those that give the desired improvement in performance.

This case study considers a pressure vessel that is required to be transported for long distances by road, across widely varying road surface conditions, shown schematically in Figure 14. For this transport condition the fatigue performance of the welded joints are most important. The fatigue performance of these welded joints is dependent on the material weld fatigue properties and the stresses calculated in the region of the weld.

For this transport condition the stresses at the welds primarily result from inertia loading. This includes the direct road induced loads, through the trailer axle suspension, and additional dynamic loads through flexing of the trailer and internal masses within the pressure vessel itself. These inertia loads can vary greatly depending on the speed the vehicle is travelling, how smooth or rough the road surface is, the stiffness of the trailer, how the pressure vessel is mounted on the trailer, and many other factors.

Computer simulations were performed to calculate the motion of the pressure vessel in response to the vehicle travelling over a speed bump. This response was used in a finite element analysis of the pressure vessel. The resulting time varying stresses were used in a weld fatigue analysis using both the seam weld method and the nominal stress method for a Class D weld according to BS7608 [6].

To implement the seam weld method for a thick welded structure modeled with solid elements requires the weld line to be identified as co-ordinates in space together with two vectors defining directions. The first vector defines the direction to ‘drill down’ into the solid elements, and the second vector defines the direction away from the weld toe. These enable the stresses to be transformed into a local reference system and calculation of the membrane and bending stresses. It is not necessary for the weld line, defined by co-ordinates in space, to correspond with nodes in the FE model, simplifying the FE modeling. These weld line co-ordinates and vectors can be obtained from the modeling software.

Contour plots of the seam weld fatigue analysis results are shown in Figure 15 and Figure 16, and results at a location of interest are shown for both calculation methods in Table 2. For this location, and with this speed bump loading, the results are almost identical. However such close agreement is considered to be coincidental, other locations and further work with more complex road surface conditions have shown differences of factors of 10 on the predicted fatigue life in cycles.

TABLE 2 – Comparison of weld fatigue damage estimates between the seam weld method and the nominal stress method.

	Seam weld life in cycles	Class D weld life in cycles
Speed bump loading	5,830,000	6,340,000

REFERENCE LIST

(1) Wöhler, A., *Über die Festigkeitsversuche mit Eisen und Stahl, Zeitschrift für Bauwesen,* V**ol. 20**, 1870, pp. 73-106.

(2) Basquin O. H., Proc. ASTM 10, 625, 1910.

(3) Matsuishi, M., Endo, T., Fatigue of Metals Subjected to Varying Stress, *Japan Society of Mechanical Engineers*, Jukvoka, Japan, 1968.

(4) Palmgren A., Die lebensdauer von kugellagern, *zeitschrift des vereinesdeutscher ingenierure*, **Vol. 68**, No. 14, 1924, pp. 339-341

(5) Miner M. A., Cumulative damage in fatigue, *J. Applied Mechanics*, **Vol. 67**, 1945, pp. A159-A164

(6) BS7608, *Fatigue Design and Assessment of Steel Structures*, BSI, England, 1993

(7) *Eurocode 3, BS EN 1993-1-9:2005*, Fatigue, BSI, 2005

(8) *ASME Pressure Vessel Code VIII Division 2*, ASME, USA, 2010

(9) The International Institute of Welding, *Stress Determination for Fatigue Analysis of Welded Components*, Abington Publishing, Cambridge, England, 1995

(10) Fermér M, Andréasson M, Frodin B., Fatigue Life Prediction of MAG-Welded Thin-Sheet Structures, SAE Technical Paper 982311, 1998

(11) FKM-Guideline, Analytical Strength Assessment, 5th edition, Forschungskuratorium Maschinenbau (FKM), 2003

(12) Gurney T. R., Fatigue of thin walled joints under complex loading, Abington Publishing (Woodhead Publishing Ltd in association with The Welding Institute), 1997

(13) Bonnen J. J. F., Mandapati R., Kang H. T., Iyengar R. M., Khosrovaneh A. K., Amaya M. A., Citrin K., Shih H. C., Durability of Advanced High Strength Steel Gas Metal Arc Welds, SAE Technical Paper 2009-01-0257, 2009.

FIGURES

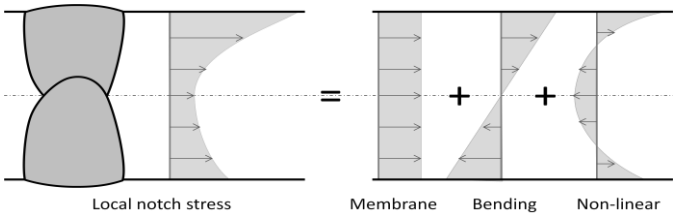

Figure 1 Local notch stress at a weld toe, comprising membrane, shell bending and non-linear stress peak

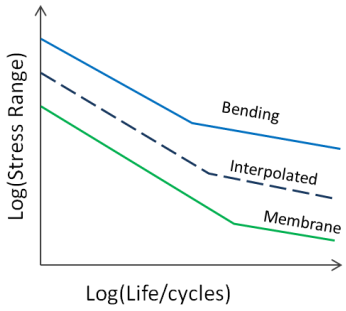

Figure 2 Interpolation between membrane and bending SN curves

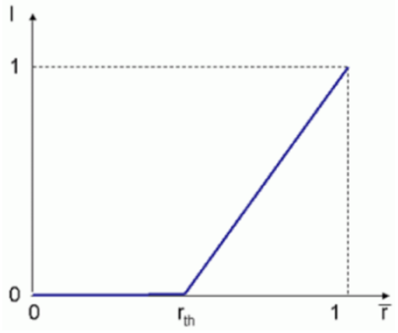

Figure 3 Interpolation function between membrane and bending SN curves

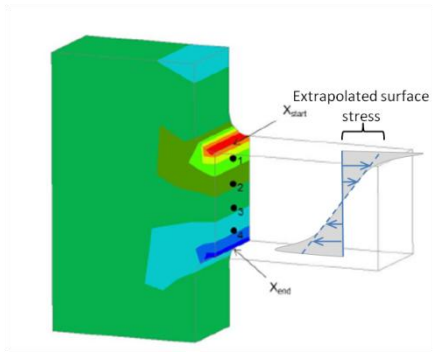

Figure 4 Through-thickness stress recovery with surface extrapolation

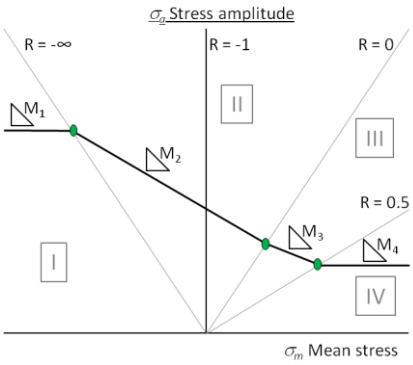

Figure 6 Haig diagram from [11] used for cycle mean stress correction

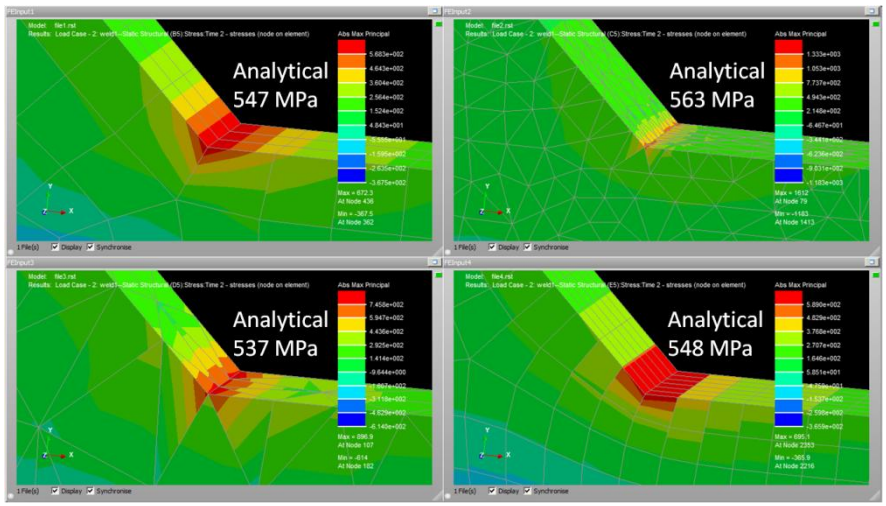

Figure 5 Investigation on mesh sensitivity to analytical extrapolated surface stresses

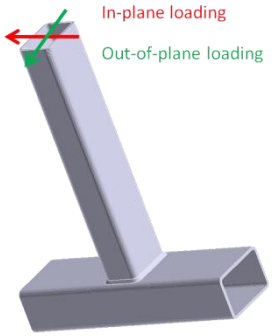

Figure 7 'T' specimen subjected to various ratios of in- and out-of-plane loading

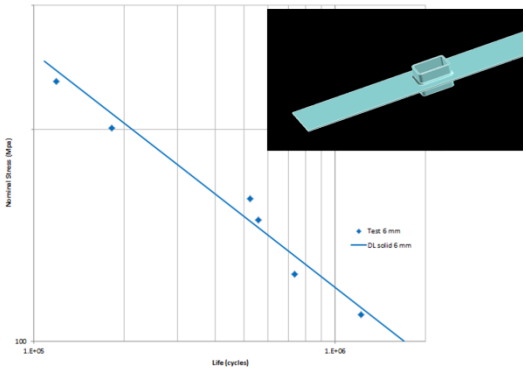

Figure 9 Comparison with TWI [12] NLC tube attachment

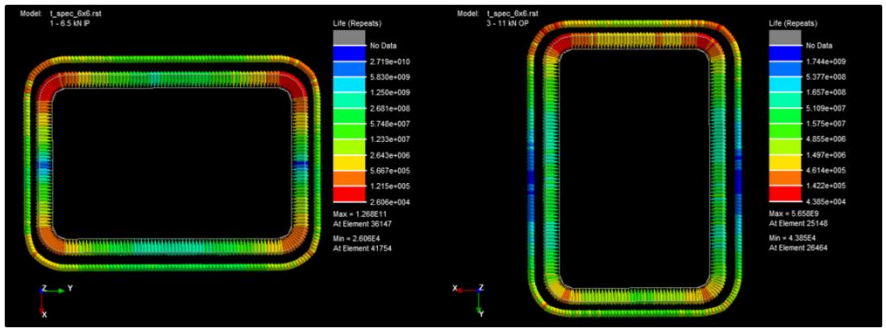

Figure 8 FEA-based fatigue analysis of 'T' coupon correctly identifying all initiation sites

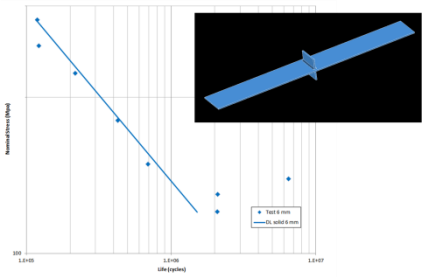

Figure 10 Comparison with TWI [12] NLC short attachment to both sides

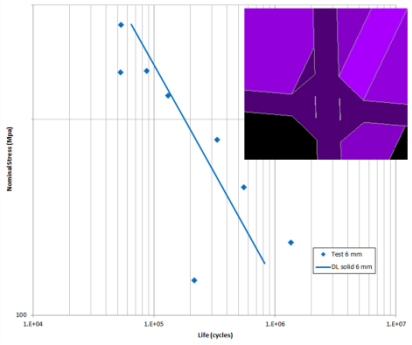

Figure 11 Comparison with TWI [12] LC short attachment

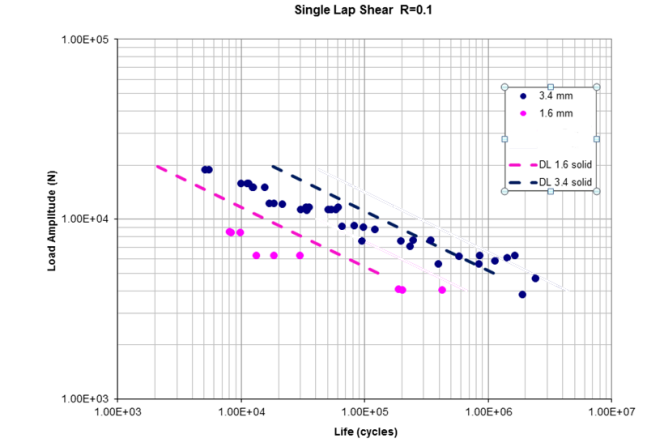

Figure 12 Comparison with Auto steel partnership [13] single lap shear joint

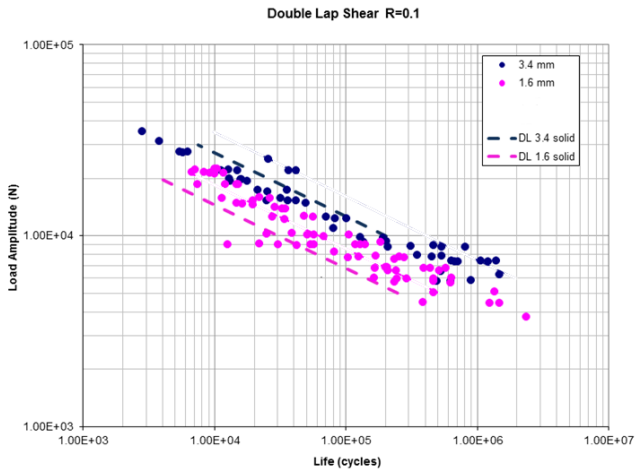

Figure 13 Comparison with Auto steel partnership [13] double lap shear joint

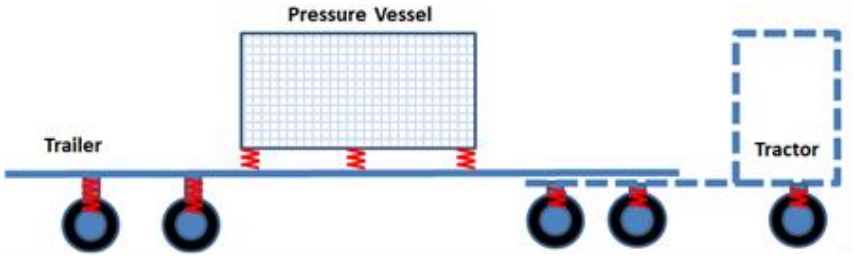

Figure 14 Schematic of the pressure vessel during road transportation

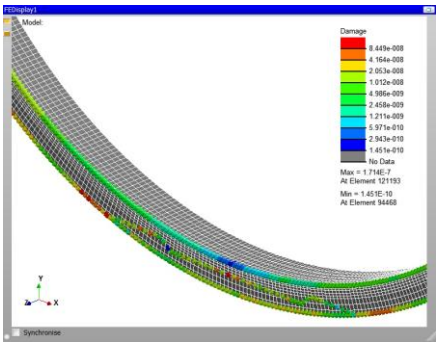

Figure 15: Weld seam damage plot

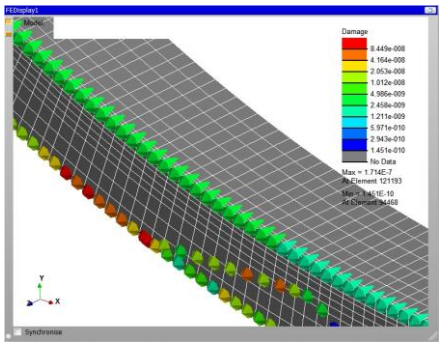

Figure 16: Close up view of damage plot